Experimental investigation on the effect of user's hand proximity on a compact ultrawideband MIMO antenna array

Zhekov, Stanislav Stefanov; Tatomirescu, Alexandru; Foroozanfard, Ehsan; Pedersen, Gert F.

Published in:
I E T Microwaves Antennas & Propagation

DOI (link to publication from Publisher):
10.1049/iet-map.2016.0054

Publication date:
2016

Document Version
Accepted author manuscript, peer reviewed version

Experimental Investigation on the Effect of User's Hand Proximity on a Compact Ultrawideband MIMO Antenna Array

Stanislav Stefanov Zhekov*, Alexandru Tatomirescu , Ehsan Foroozanfard , Gert Frølund Pedersen

Section of Antennas, Propagation and Radio Networking (APNet), Department of Electronic Systems, Aalborg University, Fredrik Bajers Vej 7, 9220 Aalborg, DK-9220 Aalborg, Denmark
*stz@es.aau.dk

Abstract: An experimental study of the interaction between user's hand and an ultrawideband multiple-input multiple-output (MIMO) antenna array is presented for mobile terminals. The dual-element array covers the frequency ranges 698-990 MHz and 1710-5530 MHz with a good efficiency in free space. Depending on the standard, it can be used for channel sensing in cognitive radio networks or for communications in cellular networks. Hand phantoms for three usage scenarios are used for the investigation, namely, personal digital assistant (PDA) right hand, PDA left hand, and two hands. The absorption in the immediate located hand is the main factor causing degradation of the total efficiency (slightly affected by the hand induced changes in the S-parameters), reduction and imbalance in the antennas mean effective gain contributing to a deteriorated diversity gain. The user caused changes in the antennas radiation patterns reduce the correlation in the lower band which enhance the diversity gain and multiplexing efficiency. The exposure of the hand in each scenario is studied by the Specific Absorption Ratio (SAR).

1. Introduction

Fixed spectrum allocation has started to become highly inefficient due to the strong variations of the data traffic across time, space and frequency. Recent studies have shown that a significant part of the licensed frequency bands remains underutilized for a long period of time [1]. This has motivated the invention of cognitive radio (CR) providing a better spectrum utilization through an approach called opportunistic spectrum sharing, which allows a dynamical access of the cognitive radio users to the licensed spectrum bands without interfering significantly the primary licensed users [2]-[4]. A cognitive radio system has two types of antennas in its front-end: 1) an ultrawideband (UWB) sensing antenna, and 2) a reconfigurable communication antenna. The UWB antenna is employed for finding idle parts of the spectrum, while the reconfigurable antenna tunes its operating frequency for communications. Different antenna designs for CR systems can be found in [5]-[7].

In mobile terminals, the UWB sensing antenna can also be employed as a communication antenna, i.e. in CR networks, the antenna is used for sensing the spectrum of interest, while in cellular networks for voice and data transfer. This can be realized by using a switch for switching the antenna between a CR and a communication chip. The introduction of more sensing antennas into the device enables an improvement in the channel sensing by using their diversity performance. Except in diversity mode for mitigating the effects of signal fading, in cellular networks and in high signal-to-noise ratio (SNR) environments such a system can also be used in spatial multiplexing

mode to increase the channel capacity. However, the realization of wideband antennas with a good performance for mobile terminals faces two problems.

The first problem is a consequence of the limited volume available for the deployment of multiple antennas in handsets. This greatly hinders the achievement of requirements for multi-antenna terminals in terms of wide bandwidth, high efficiency and low correlation. In recent years, different designs of wideband antenna arrays for mobile terminals have been proposed. Table 1 presents a comparison between the employed antenna array and some other dual-antenna structures. All geometric features are given in λ_m, which is the wavelength at the lowest operating frequency of the corresponding antenna. The size of radiator in the presented array is similar to that of the other 3D antennas in [8] and [10]. The presented system has the smallest cutback area under each antenna and one of the smallest ground plane and PCB area in wavelengths. The covered bands of the antennas in [8] (which also start at 698 and 1710 MHz) are narrower than these of the presented antennas, but the radiation efficiency has higher maximum value over the band 1710-290 MHz. In addition, if the electrical size of the structure is big then it is easier to obtain both large bandwidth and high efficiency.

Table 1 Comparison between the performance of the presented antenna array and several other compact broadband dual-element antennas for mobile devices reported in the literature.

Ref. work	Present work	[8]	[9]	[10]	[11]
Single antenna size	0.068x0.039 x0.012 (xλ_m^3)	0.082x0.026 x0.012 (xλ_m^3)	0.101x0.083 (xλ_m^2)	0.089x0.068 x0.005 (xλ_m^3)	0.144 x 0.12 (xλ_m^2)
Cutback area	0.003 (xλ_m^2)	0.004 (xλ_m^2)	0.014 (xλ_m^2)	0.014 (xλ_m^2)	0.023 (xλ_m^2)
Ground plane	0.032 (xλ_m^2)	0.019 (xλ_m^2)	0.181 (xλ_m^2)	0.074 (xλ_m^2)	0.153 (xλ_m^2)
PCB area	0.038 (xλ_m^2)	0.027 (xλ_m^2)	0.209 (xλ_m^2)	0.101 (xλ_m^2)	0.199 (xλ_m^2)
BW (MHz)	698-990 1710-5530	698-960 1710-2690	1850 - 5150 5850-11190	1700-2700 4700-8500	2400-6550
Rad. eff. (%)	54-79 31-84	30-70 40-92	N/A	59-70 59-90	52-94
Tot. eff. (%)	39-58 23-80	N/A	71-92 71-89	N/A	47-73

The second and inevitable issue results from the inherent operation of the mobile terminal in a proximity to the user, usually located in the antenna near-field. The user presence changes the antenna radiation pattern and since the human tissue is a lossy dielectric material it affects the antenna performance by absorbing a portion of the power (reduce the radiation efficiency) and by shifting the resonance frequency due to the introduced dielectric loading (changes the input impedance and bandwidth of the antenna) [12]-[15]. The hand position and grip have a different effect on the antenna performance [16]-[18]. The degradation of the antenna total efficiency and mean effective gain deteriorates the reliable operation of the system as the effect is more significant when the user is closer to the antenna. In multi-antenna systems, the user proximity has an influence on the envelope correlation, diversity gain and multiplexing efficiency [19]-[21]. However, most researches have only been focused on a single hand impact and hereof the scenarios with two hands have not been well investigated. Furthermore, there is little research about the user hand effect on antennas broadband enough to be used for both sensing and communications and also on antennas operating above 2700 MHz.

This paper presents an experimental study of the interaction between the user's hand and con-

crete design of a dual-element UWB antenna array for handsets. The antenna system has been presented in our previous work [22]. The influence of three different hand phantoms on the antennas performance is investigated and the analysis is focused on S-parameters, feeding efficiency, absorption efficiency, total efficiency, radiation pattern, mean effective gain, branch power ratio, envelope correlation, diversity gain and multiplexing efficiency. Additionally, the SAR of the antennas in all usage scenarios is studied.

2. MIMO Antenna Array Design

The geometry of the antenna array is shown in Fig. 1 [22]. It is composed of two identical antennas featuring with both wide bandwidth and good total efficiency. However, there is always a tradeoff between size and performance. The compactness is needed due to the limited available space in handsets for integrating multiple antennas. For CR is necessary the sensing antenna to be wideband to 'sense' broad spectrum and also to have a good efficiency for provision of a good search sensitivity. The use of more (diversity) antennas additionally improves the quality of channel sensing by mitigating the effect of fading. Since the antenna system covers most of the LTE bands it can also be used for cellular communications and the two antennas can operate in spatial multiplexing mode or diversity mode depending on the SNR level.

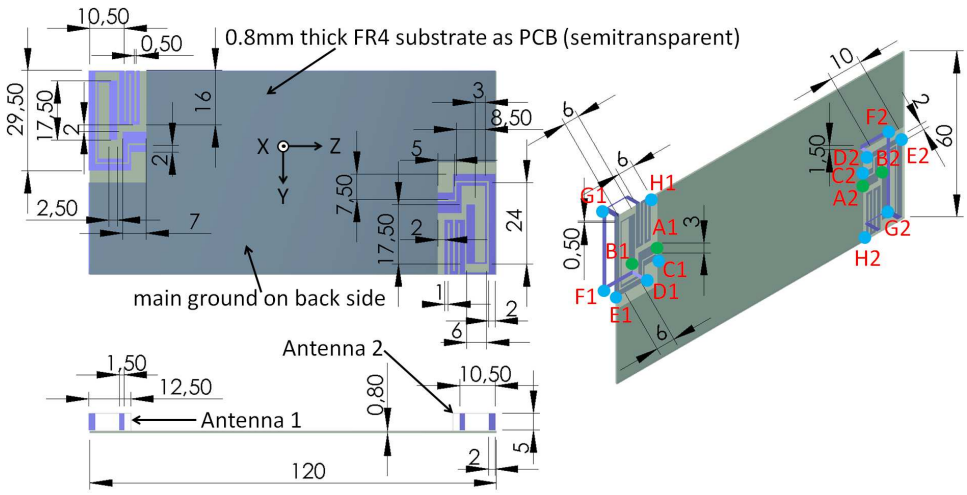

Fig. 1. *Geometry of the antenna array without the casing [22]*

The antenna structure is an off-ground type, which generally enables the achievement of a wider bandwidth than the on-ground type when comparing antennas with a similar size. Each antenna has a total volume of 29.5 x 17 x 5 mm^3 and the antennas are placed diagonally since for this design this arrangement provides a lower envelope correlation. The PCB is made of a 0.8 mm thick FR4 substrate with a planar area of 120 x 60 mm^2. As a model of the mobile phone casing is used a 1 mm thick plastic cover with a total volume of 124 x 64 x 10 mm^3. The ground plane is printed on the back side of the PCB and the cutback area under each antenna is 33 x 17 mm^2. The antennas are formed by two elements - a driven strip monopole (A1-B1/A2-B2) and a parasitic shorted strip (C1-D1-E1-G1-H1/C2-D2-E2-G2-H2). The driven monopoles are excited at points A1 and A2, and the parasitic strips are short circuited at points C1 and C2 for antenna 1 and antenna 2, respectively. The length of the driven monopoles is 68.5 mm which is around 0.25

wavelength at 1110 MHz but this fundamental resonance frequency is lowered when the shorted strips are introduced due to the coupling between the two types strips. The parasitic strips have a length of 120 mm which is around 0.25 wavelength at 625 MHz. To each of them is introduced an additional line (D1-F1-G1/D2-F2-G2) with length of 40 mm for an enlargement of the impedance bandwidth. The excitation of the parasitic strips is by an electromagnetic coupling to the driven monopoles.

It should be noted about the results presented in the rest of the paper, that the S-parameters are measured by using Agilent N5227A PNA network analyzer [23], while the radiation properties by using the antenna measurement equipment Satimo StarLab [24]. To ensure that the antennas positions with respect to the hand are not changed (which otherwise leads to different antenna performance), the prototype is placed in the phantom and all measurements are conducted, as the switching from S-parameters (also measured in the anechoic chamber) to radiation properties measurements is done carefully without moving the prototype. In addition, ferrite beads are used in order to choke the current flowing on the outer surface of the cables.

2.1. Free Space Performance of the Antenna Array

The measured S-parameters are shown in Fig. 2(a), and the prototype is presented in Fig. 3(a). For mobile phones S_{11}(S_{22}) around and below -6 dB is considered acceptable, since this value provides a sufficiently low mismatch loss. The lower frequency band 698-990 MHz is covered by combining two resonance modes, one at around 750 MHz (fundamental of the parasitic strip) and the other one at 950 MHz (fundamental of the driven monopole). Seven higher-order modes (at 2070, 2470, 2830, 3210, 3610, 4890 and 5320 MHz) generated by either driven monopole or parasitic strip are incorporated to cover the higher frequency band 1710-5530 MHz. The measured S_{21} is around and below -10 dB (required for mobile terminals) which ensures a low coupling loss.

The total efficiency η_{tot} of an antenna is defined by:

$$\eta_{tot} = \eta_{rad}\eta_{feed} \tag{1}$$

where η_{rad} is the radiation efficiency and η_{feed} is the feeding efficiency of the antenna. In the case of a dual-element array, the feeding efficiency is given by:

$$\eta_{feed1(2)} = (1 - |S_{11(22)}|^2 - |S_{21(12)}|^2) \tag{2}$$

which is used to determine losses due to the reflection at the antenna input port and the coupling between the antennas.

The measured total efficiencies are shown in Fig. 2(b). The antennas have a total efficiency above 38 % and 24 % over the lower and higher band, respectively. This indicates a good performance despite their compactness. The calculated feeding efficiencies are shown in Fig. 2(c). Since the isolation is below -10 dB, then the main factor leading to a reduction of the feeding efficiency and therefore of the total efficiency is the return loss. The calculated radiation efficiencies ($\eta_{rad1(2)} = \eta_{tot1(2)}/\eta_{feed1(2)}$) of the antennas shown in Fig. 2(d) have minimum value of 55 % and 31 % over the lower and higher band, respectively. The differences in the corresponding parameters between the antennas are due to the manufacturing inaccuracies and measurement errors.

3. Investigation on the Effect of the User's Hand

Three usage scenarios were investigated, namely, data mode with PDA right hand, data mode with PDA left hand, and landscape mode with two hands. The positions of the prototype with

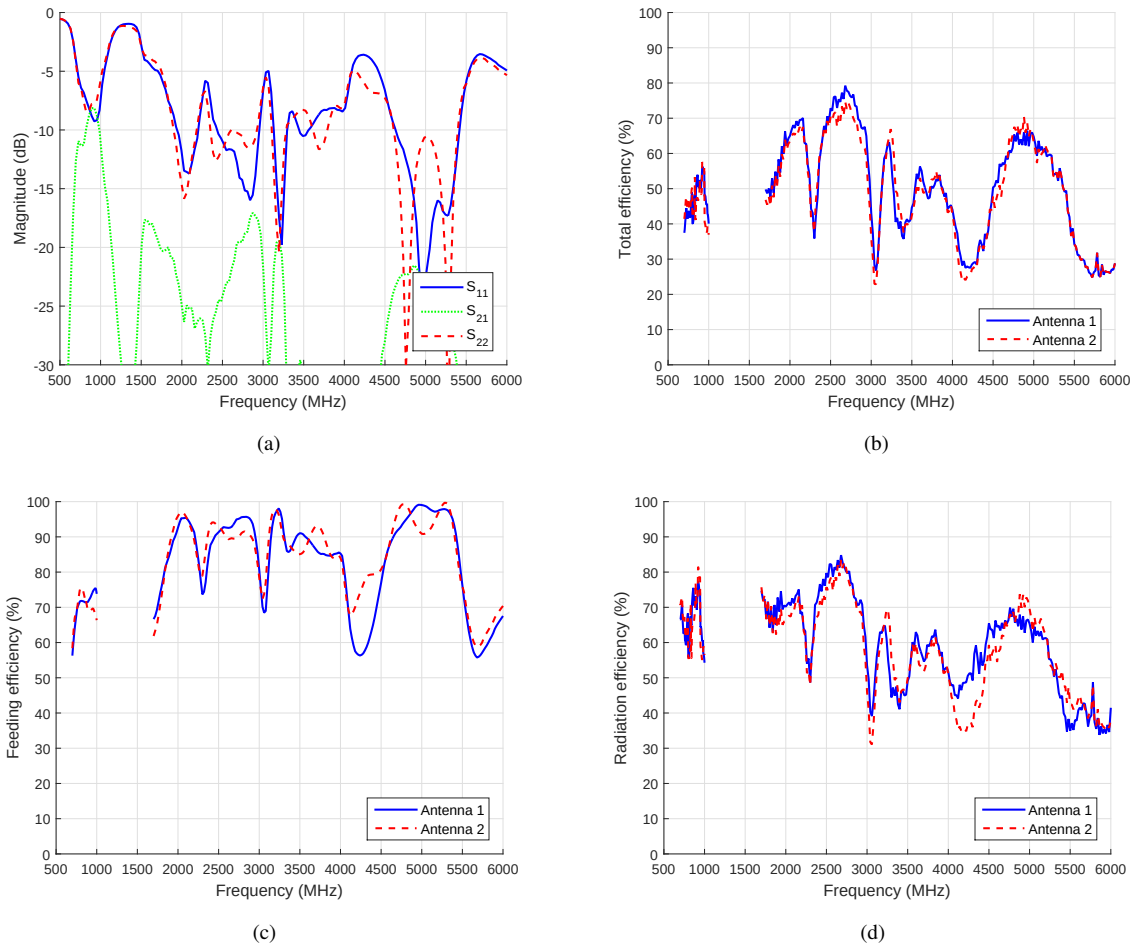

Fig. 2. *Free space scenario*
a Measured S-parameters of the antennas
b Measured total efficiency of the antennas
c Calculated feeding efficiency of the antennas
d Calculated radiation efficiency of the antennas

respect to the right and left hand phantom are in accordance with the CTIA standard revision 3.4.2 [25]. Since the landscape mode is not standardized, the mockup was positioned in the hands in a common holding manner.

In a typical usage scenario the user holds the mobile terminal and therefore, if the effect of the immediately located hand is taken into account when designing the antenna, part of the degradation in its performance can be avoided. Generally, users hold the mobile terminals in a widely variable way and the degree of hand impact depends on the antenna (design, size, location and near field distribution) and the grip (position of the fingers with respect to the antenna, obstructed antenna area and palm-handset distance). However, the employment of two antennas gives the opportunity if the user significantly affects one of them then the other one to be utilized.

Each antenna element of the system contains a loop (D1-E1-G1-F1 for antenna 1 and D2-E2-G2-F2 for antenna 2) and these loops have two functions. Firstly, the loop improves the impedance matching and enlarges the bandwidth of the antennas. Secondly, it makes the antennas more robust

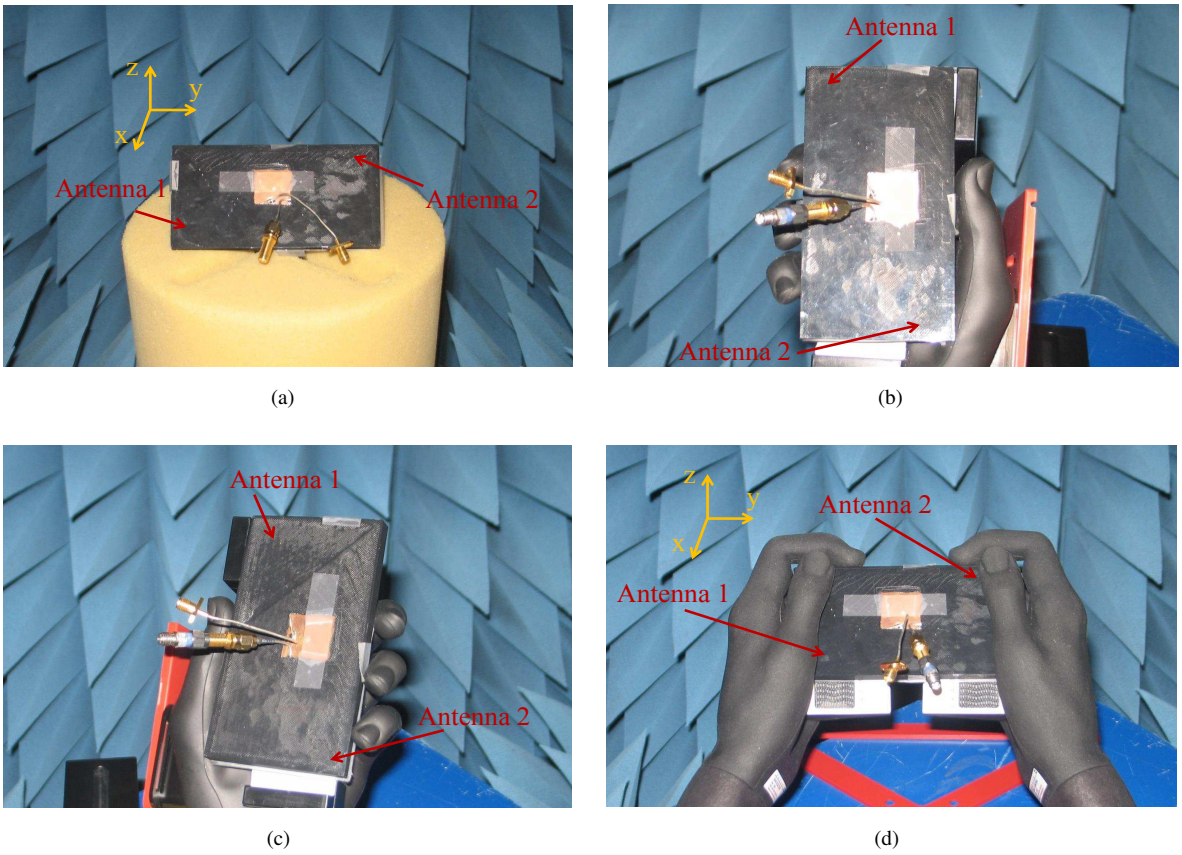

Fig. 3. *Four different scenarios for antennas performance evaluation*
a Free space
b PDA right hand (data mode)
c PDA left hand (data mode)
d Two hands (landscape mode)

against the hand effect. The human tissue has a dielectric permittivity (responsible for the lowering of the resonant frequency) and an electrical conductivity (leads to energy dissipation, i.e. losses), and it affects the electric fields. However, the loop antennas have a relatively weak electric field and strong magnetic field in the near zone. Thus, the introduction of the loop relieves the influence of tissue permittivity and conductivity on the antenna performance and makes the antenna less sensitive to the hand proximity.

In recent years different techniques for mitigating the user hand effect have been proposed. A suppression of the effect can be obtained by using a thick buffer layer insulating the antenna and the human tissue made of a high permittivity dielectric with low conductivity (low loss) [18]. Such materials allow reducing the antenna size, antenna near-field to be confined and to increase the electrical distance to the user. Thus, the effect of the user hand can be decreased, but is needed to sacrifice antenna volume by making room for a buffer layer. Also, the loading with high permittivity materials lowers the resonance frequency and can reduce the bandwidth of the antenna [18]. Another method for reducing the user influence on a single antenna has been proposed in [15]. However, even for a single antenna the technique is based on the use of two identical non-

self-resonant antennas placed one over the other on the edge of the PCB and pointing in opposite directions. Thus, in data mode the antenna directed opposite to the index finger is selected, since it is less affected by the hand and the other one operates as a shield [15]. A disadvantage is the narrow bandwidth of the antennas and that the implementation of this technique for wideband antennas is complicated. The deployment of four identical antennas at the four corners of the PCB and dynamically selecting the one(s) less affected by the user hand can be used for improving the performance of the mobile terminal [21], [26]. However, the integration of many antennas requires either increasing the size of the PCB or reduction of the antennas size which inevitably affects the efficiency and bandwidth (especially at low frequencies where the antennas have to be larger). In addition, the latter two techniques will not improve significantly the mobile phone performance in landscape mode due to the large hand coverage of all antennas, i.e. the antennas will have a similar performance.

3.1. Right Hand Scenario

The right hand phantom and the antennas positions are presented in Fig. 3(b). The measured S-parameters are shown in Fig. 4(a). The dielectric loading introduced by the hand located in the antenna near field lowers the antenna resonance frequencies and therefore changes its input impedance and operating bandwidth. The degree of impact depends on the position of the antenna with respect to the user's hand as well as the operating frequency. Comparing results in Fig. 4(a) with these in free space (see Fig. 2(a)) one can see, that at low frequencies the phantom has a greater impact on the input impedance of antenna 2. The difference in the matching is a consequence of the different positions of the antennas with respect to the phantom and the presence of more tissue around antenna 2 results in a larger change of S_{22} and extension of the covered lower band. At high frequencies the difference between S_{11} and S_{22} is small. The S_{21} is below -10 dB and is improved compared to free space.

The total efficiency of each antenna in the vicinity to a user can be defined as:

$$\eta_{tot} = \eta_{rad}\eta_{abs}\eta_{feed} \tag{3}$$

where η_{rad} is free space radiation efficiency and η_{abs} is absorption efficiency. If it is assumed that the current distribution is not significantly changed in the user presence, then η_{abs} gives the percentage of the radiated power which is not absorbed by the user.

The measured total efficiencies in this scenario are shown in Fig. 4(b). As one can see, antenna 1 exhibits a better performance. The calculated feeding efficiencies are shown in Fig. 4(c). Due to the fact that the isolation is low then the return loss is the parameter mainly controlling the feeding efficiency (except for antenna 2 in the lower band). The higher S_{11} results in a lower feeding efficiency of antenna 1 in the lower band, while in the higher band both antennas show similar performance. Fig. 4(d) shows the calculated absorption efficiencies ($\eta_{abs} = \eta_{tot}/\eta_{rad}\eta_{feed}$). The peaks in the absorption efficiency appear at the frequencies where the total efficiency has values close to these of the combination feeding efficiency-free space radiation efficiency. The more human tissue around antenna 2 results in a lower absorption efficiency, i.e. in a higher power absorption. An inspection of the results in Fig. 4(c) and (d) reveals that the higher total efficiency of antenna 1 is a consequence of the lower hand absorption.

3.2. Left Hand Scenario

The left hand scenario is presented in Fig. 3(c). The measured S-parameters are shown Fig 5(a) and as in the right hand case the input impedance of antenna 1 is less affected since it is close to

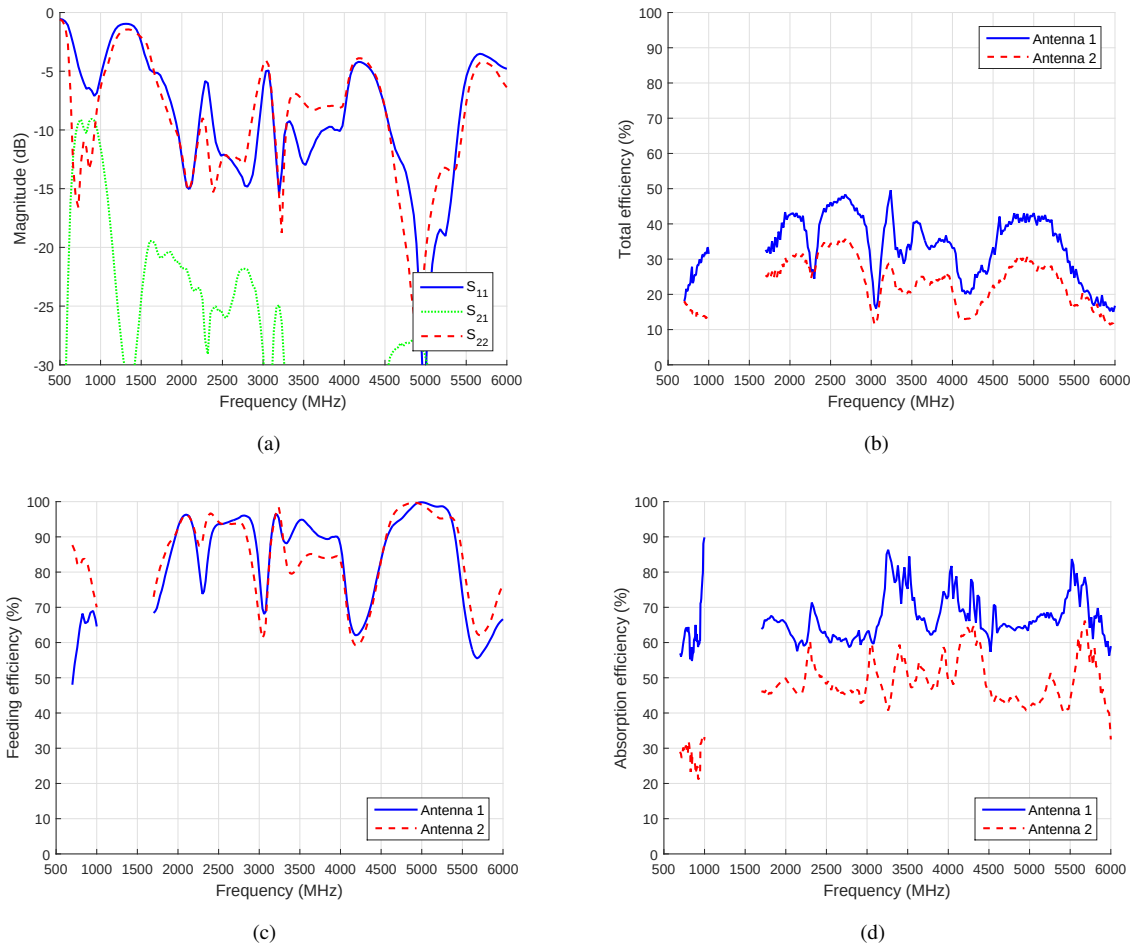

Fig. 4. *Right hand scenario*
a Measured S-parameters of the antennas
b Measured total efficiency of the antennas
c Calculated feeding efficiency of the antennas
d Calculated absorption efficiency of the antennas

the index finger while antenna 2 is covered by the palm. Also, the difference in the matching of the corresponding antennas in right and left hand scenario is small. Additionally, S_{21} is below -10 dB providing a low coupling loss.

Fig. 5(b) shows the measured total efficiencies. As expected antenna 2 exhibits a worse performance. In the lower band, due to the lower S_{22} antenna 2 has a better feeding efficiency, while in the higher band the difference between the two antennas is not significant as seen in Fig. 5(c). However, the absorption efficiencies in Fig. 5(d) indicate that antenna 2 is more affected. Therefore, the reason for the lower total efficiency of antenna 2 is the higher absorption in the human tissue. In addition, the differences between the three types of efficiency in left and right hand scenario are small. In other words, holding with right or left hand does not cause large changes in the antennas performance. Due to this, the mirroring of the antennas will not lead to an improvement, since simply antenna 1(2) in right hand will have the same performance as now in left hand and vice versa.

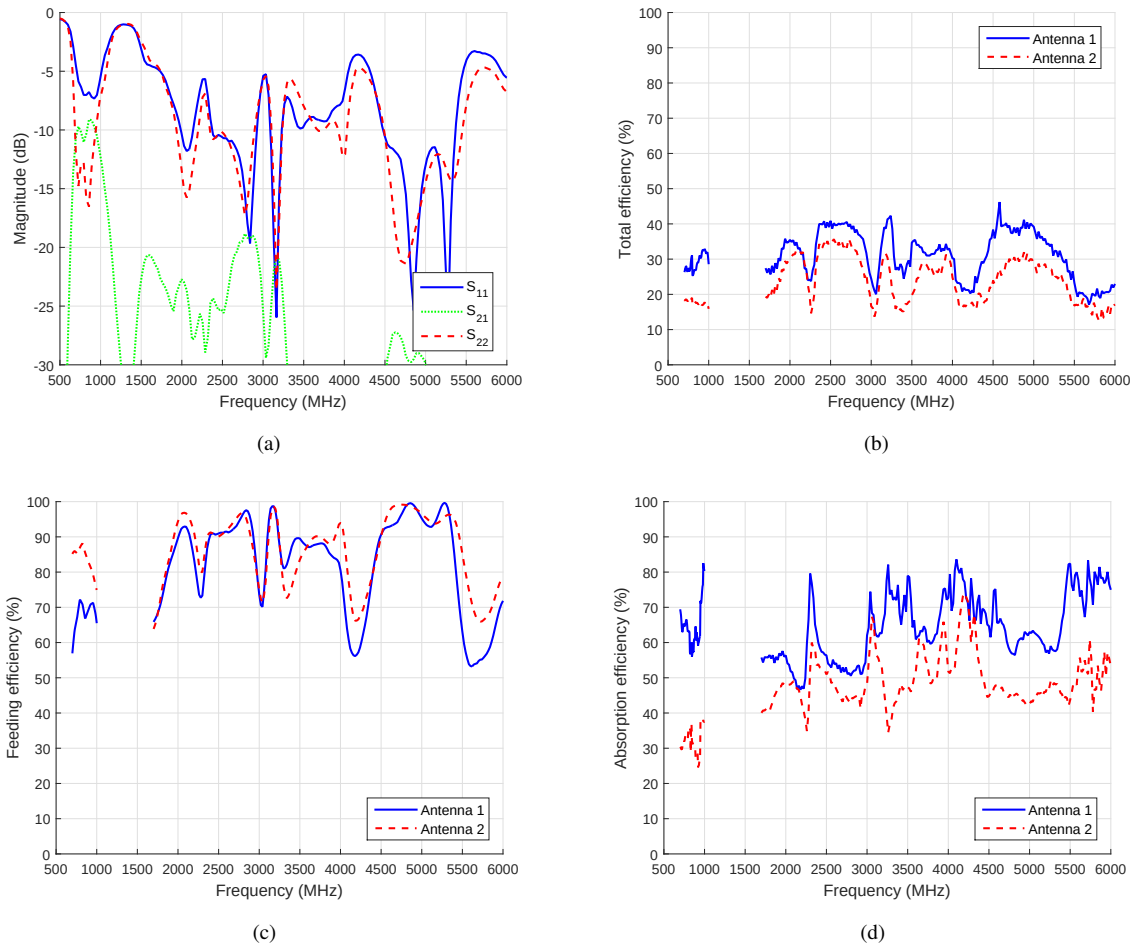

Fig. 5. *Left hand scenario*
a Measured S-parameters of the antennas
b Measured total efficiency of the antennas
c Calculated feeding efficiency of the antennas
d Calculated absorption efficiency of the antennas

3.3. Two Hands Scenario

The two hands scenario is presented in Fig. 3(d). Antenna 1 is in contact with the palm, ring finger and pinky, while antenna 2 is touched by the thumb, index and middle finger. The measured S-parameters (Fig. 6(a)) show that for both antennas the lower operating band is shifted to the left, while the high band matching is improved compared to the other three cases. The S_{21} exhibits a maximum value of -14 dB as the improved isolation compared to the other scenarios is due to the large coverage of the antenna system with a lossy tissue absorbing a significant portion of the near field energy.

The total efficiencies of the antennas (Fig. 6(b)) show maximum difference of around 5 % and around 9 % over the lower and higher band, respectively. The low total efficiency is a consequence of the firm grip and the presence of more tissue around the antennas than in the right and left hand case. The reduction of the total efficiency at low frequencies is a combination of both gradually

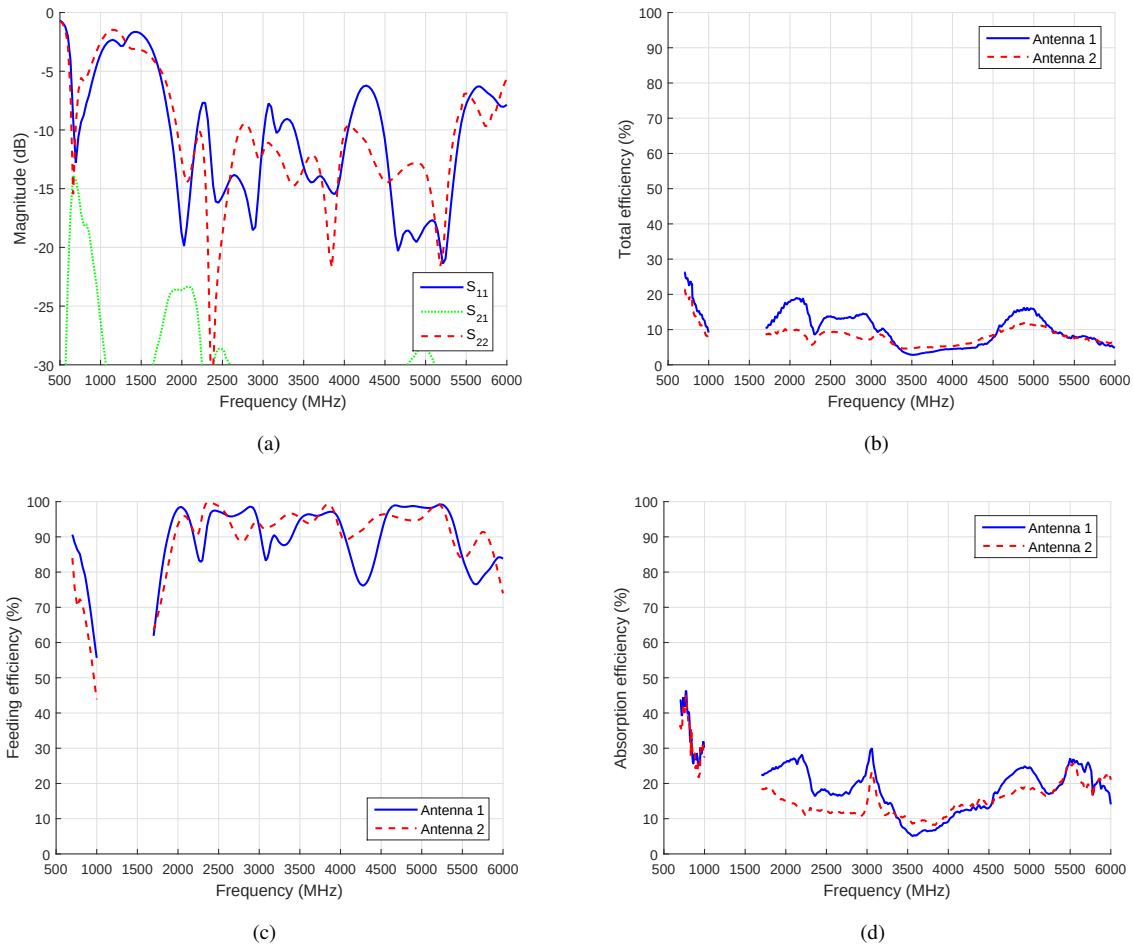

Fig. 6. *Two hands scenario*
a Measured S-parameters of the antennas
b Measured total efficiency of the antennas
c Calculated feeding efficiency of the antennas
d Calculated absorption efficiency of the antennas

decreasing feeding efficiency (Fig. 6(c)) and absorption efficiency (Fig. 6(d)). At high frequencies, the feeding efficiency of each antenna is higher than that in data mode and the main mechanism leading to a degradation of the total efficiency is the large absorption in the phantoms. Also, the mirroring of the antennas will not improve the performance of the device, since antenna 1(2) will just operate as antenna 2(1).

Fig. 7 shows the measured 3D radiation patterns at 900 MHz of the antenna array in free space and in two hands scenario (the axes are shown in Fig. 3(a), (d)). In free space the radiation patterns of the antennas have almost 'donut' shape but the directions of maximum radiation are pointing oppositely. The presence of the hands leads to a significant distortion of the patterns through shadowing and reflection/scattering. Due to the different position of the antennas with respect to the phantoms their radiation patterns are differently affected. In the proximity to the hands the patterns separate and become slightly more directive as in this scenario antenna 2 shows higher maximum directivity. Also, nulls appear at the position of the hands and a back-radiation for both

antennas is observed.

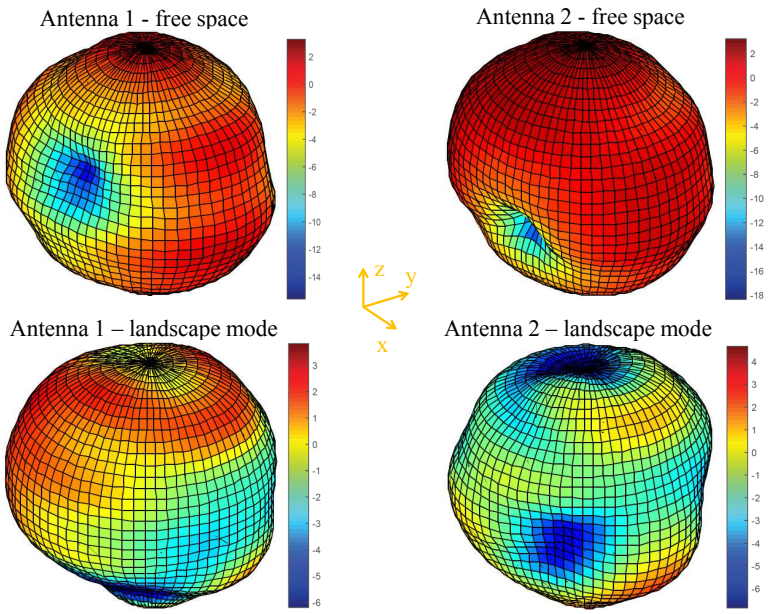

Fig. 7. *Measured 3D radiation patterns of each antenna at 900 MHz in free space and in landscape mode*

3.4. Envelope Correlation, Mean Effective Gain, Diversity Gain and Multiplexing Efficiency

The complex correlation coefficient (defines the independence of the received signals) can be calculated from the measured 3-D radiation patterns as [27]:

$$\rho_{c,ij} = \frac{\int_0^{2\pi}\int_0^{\pi} A_{ij}(\theta,\phi)sin\theta d\theta d\phi}{\int_0^{2\pi}\int_0^{\pi} A_{ii}(\theta,\phi)sin\theta d\theta d\phi \int_0^{2\pi}\int_0^{\pi} A_{jj}(\theta,\phi)sin\theta d\theta d\phi} \tag{4}$$

where $A_{ij} = XPRE_{\theta i}(\theta,\phi)E^*_{\theta j}(\theta,\phi)P_\theta(\theta,\phi) + E_{\phi i}(\theta,\phi)E^*_{\phi j}(\theta,\phi)P_\phi(\theta,\phi)$, E_θ and E_ϕ are the θ and ϕ polarized complex E-field patterns of the antennas, respectively. * denotes the complex conjugate and the indexes i,j indicates the two antennas 1,2. $P_\theta(\theta,\phi) = P_\theta(\theta)P_\theta(\phi)$ and $P_\phi(\theta,\phi) = P_\phi(\theta)P_\phi(\phi)$ are θ and ϕ polarized components of the statistical angular power density functions in elevation and azimuth of the incoming plane waves. Both $P_\theta(\theta,\phi)$ and $P_\phi(\theta,\phi)$ satisfy the condition $\int_0^{2\pi}\int_0^{\pi} P_\theta(\theta,\phi)sin\theta d\theta d\phi$=$\int_0^{2\pi}\int_0^{\pi} P_\phi(\theta,\phi)sin\theta d\theta d\phi$=1 which is the normalized power distribution for each polarization. The XPR is cross-polarization ratio of the environment and is defined by the ratio of mean incident θ to mean incident ϕ polarized power in the environment. The envelope correlation coefficient is $\rho_{e,ij} \approx |\rho_{c,ij}|^2$ [19], [27].

For an uniformly distributed isotropic environment $P_\theta(\theta,\phi) = P_\phi(\theta,\phi)$ =1/4π, the amplitudes of the incident plane waves are equal for all angles and XPR=1 [19]. For studying the user hand effect regardless of a non-isotropic environment, an isotropic environment is employed. The calculated envelope correlation coefficients in each scenario for an isotropic incoming power spectrum are shown in Fig. 8. In the lower band the user proximity reduces the correlation coefficient below 0.7. The explanation is that the user hand alters the radiation patterns of the antennas and thus

introduces more difference between them than in free space. Therefore, if the correlation is high at low frequencies in free space, the user will reduce it. In the higher band, the distance between the antennas compared to the wavelength is large enough for providing a low level of correlation.

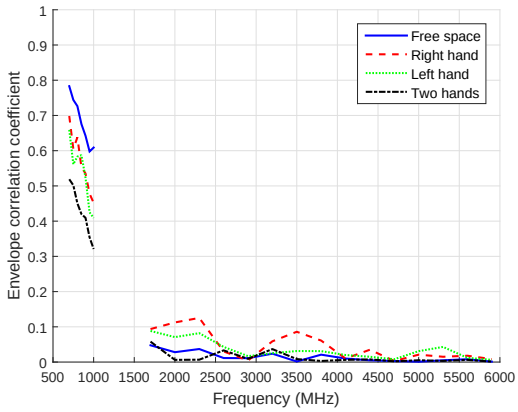

Fig. 8. *Calculated envelope correlation coefficients in all scenarios*

The mean effective gain (MEG) is defined as the ratio of the mean received power of the antenna to the total mean incident power. It is a statistical measure of the antenna gain in the mobile environment and combines the radiation performance of the antenna with the propagation characteristics of the surrounding environment, i.e. it is an average of the gain over different directions using incident radiation given by a random environment [19], [28]. The MEG can be calculated as [28]:

$$MEG = \int_0^{2\pi} \int_0^{\pi} \left(\frac{XPR}{1+XPR} G_\theta(\theta,\phi) P_\theta(\theta,\phi) + \frac{1}{1+XPR} G_\phi(\theta,\phi) P_\phi(\theta,\phi) \right) sin\theta d\theta d\phi \quad (5)$$

where $G_\theta(\theta,\phi)$ and $G_\phi(\theta,\phi)$ are the θ and ϕ polarized components of the antenna power gain pattern, respectively. For an isotropic environment (used in the study), the MEG is equal to 0.5 (-3 dB) of the antenna total efficiency.

The branch power ratio (BPR) is defined as:

$$BPR = \frac{MEG_1}{MEG_2} \quad (6)$$

where MEG_1 and MEG_2 are the MEGs of the two antennas. The achievement of a good diversity performance requires BPR close to 1 (0 dB).

Table 2 presents the MEGs and BPRs in all scenarios. As expected, the best results are obtained in free space. The vicinity of the user hand leads to a degradation of the MEG and increasing of the BPR (unequal branch signals). In data mode, antenna 2 suffers from a higher reduction in the total efficiency, due to the presence of more human tissue around it (larger absorption), and therefore in the MEG. The lowest MEGs are obtained in landscape mode and the large drop in the performance is caused by the firm grip of the phantoms (large coverage of the radiators) leading to a significant degradation of the total efficiency by absorption. The highest BPR (the largest difference in the MEG of the antennas) is realized in right hand scenario at 900 MHz, but except this case the BPR is below 3 dB.

The diversity gain (DG) is defined as the improvement in the SNR gained from combining signals from a set of diversity antenna elements (SNR from the combined signal) relative to the SNR from the best single antenna element [20]. For a selection combiner with two ideal antennas (total efficiency 100 %, envelope correlation=0 and power levels of the signals received by the antennas are the same) the DG is 10 dB for the probability that the SNR will fall below a certain threshold of 1 % (radio link reliability is 99 %) [11], [27]. To achieve a DG as high as in the ideal case, both correlation and difference between the power levels of the signals received by the two radiators (or BPR) should be low. The increasing of the envelope correlation results in decreasing diversity effectiveness. This DG degradation caused by the envelope correlation (for values not too close to 1) is given by the factor [27]:

$$DF = \sqrt{1 - \rho_e} \tag{7}$$

The influence of the difference between the power levels (power imbalance) of the signals delivered by the antennas on the reduction of the DG can be accounted by using the minimum BPR as [27]:

$$K = min\left(\frac{MEG_1}{MEG_2}, \frac{MEG_2}{MEG_1}\right) \tag{8}$$

Based on the above consideration, the DG of a dual-element antenna array can be calculated as [11]:

$$DG = DG_0.DF.K \tag{9}$$

where DG_0=10 dB is for a selection combiner with two ideal antennas for 1% probability [27]. The DG defined in this way tends to compare a real diversity antenna system ($\rho_e \neq 0$ and BPR$\neq$0 dB) with an ideal (not-realistic) antenna system in free space (no user interaction).

The DGs of the array in all scenarios is shown in Table 2. The lowest DG is 4.86 dB (or 5.14 dB less compared to that of an ideal system), obtained in the right hand scenario at 900 MHz. Since the BPR is higher, then the lower correlation in landscape mode at 900 MHz is the reason for the higher DG compared to free space. The higher correlation and BPR (except the BPR for the two hands scenario) in the lower band compared to the higher band are the reason for the lower DG. At high frequencies the DG of the antenna array in free space is very close to that of an ideal system. Generally, the antenna system has an acceptable diversity performance in all scenarios.

In [29], the multiplexing efficiency (ME) has been introduced as a parameter for evaluating the performance of MIMO antenna arrays in spatial multiplexing mode of operation in an isotropic environment. The ME considers the impact of the total efficiencies of antenna elements, efficiency imbalance and envelope correlation on the multiplexing performance. In general, the ME determines the loss of efficiency in SNR when using a real antenna array in an isotropic environment to achieve the same channel capacity as that of an ideal antenna array (100% efficient and decorrelated antennas) in the same isotropic environment. Assuming a high SNR isotropic environment, ME for a dual-element array can be calculated as [29]:

$$ME = \sqrt{(1 - \rho_e)\eta_1\eta_2} \tag{10}$$

where η_1 and η_2 are the total efficiencies of the antennas. Table 2 shows the MEs in all scenarios. Over the lower band, the reduction of the total efficiencies of the antennas due to the user proximity can not be compensated by the lower correlation in the user cases and therefore the ME decreases

Table 2 Mean effective gain, branch power ratio, diversity gain and multiplexing efficiency of the antennas

Free space					
Frequency (MHz)	MEG_1 (dB)	MEG_2 (dB)	BPR (dB)	DG (dB)	ME (dB)
900	-5.86	-6.09	0.23	7.53	-5.21
2500	-4.38	-4.52	0.14	9.83	-1.47
5000	-4.89	-4.99	0.1	9.89	-1.95
Right hand					
Frequency (MHz)	MEG_1 (dB)	MEG_2 (dB)	BPR (dB)	DG (dB)	ME (dB)
900	-8.37	-11.55	3.18	5.15	-8.62
2500	-6.36	-7.63	1.27	8.66	-4.07
5000	-6.65	-8.44	1.79	8.17	-4.59
Left hand					
Frequency (MHz)	MEG_1 (dB)	MEG_2 (dB)	BPR (dB)	DG (dB)	ME (dB)
900	-8.18	-10.73	2.55	5.84	-8.06
2500	-6.88	-7.59	0.71	9.19	-4.06
5000	-7.07	-8.43	1.37	8.53	-4.84
Two hands					
Frequency (MHz)	MEG_1 (dB)	MEG_2 (dB)	BPR (dB)	DG (dB)	ME (dB)
900	-11.48	-12.51	1.03	7.82	-10.14
2500	-11.60	-13.24	1.64	8.28	-9.49
5000	-11	-12.47	1.47	8.52	-8.74

compared to free space. The most critical is the landscape mode where eventhough the correlation is the lowest, the firm grip leads to the most significant degradation of the total efficiencies and thus in ME. At 2500 and 5000 MHz both higher efficiencies and lower correlations than at 900 MHz provide better MEs in all scenarios.

3.5. Specific Absorption Rate

The simulated SAR values of the antennas for all user cases (by using CST Microwave Studio [30]) are shown in Table 3. Following the ICNIRP guidelines applied in Europe, the SAR is averaged over a 10 g volume of tissue and the maximum allowed SAR for hand is 4 W/kg [31]. In the study, the input power of each antenna is set to 23 dBm (0.2 W), which is the maximum emission power for LTE handsets regardless of the operating frequency. It should be noted that in landscape mode the used computer model slightly differs from the phantoms employed in the measurements. The data reveals that antenna 1 has smaller a SAR for both right and left hand than antenna 2 since it is further away from the hand, while antennas 2 is in the proximity of the hand palm. In the higher band, the SAR of both antennas in landscape mode exceed 4 W/kg. The high values are due to the firm grip (small distance antenna-phantom) and the high maximum emission power.

Table 3 Simulated SAR values of the antennas

Frequency (MHz)	SAR (W/kg)					
	Right hand		Left hand		Two hands	
	Antenna 1	Antenna 2	Antenna 1	Antenna 2	Antenna 1	Antenna 2
900	0.31	0.92	0.34	0.91	1.17	1.38
2500	1.41	2.31	1.17	2.54	4.28	4.67
5000	1.75	3.76	1.44	3.58	4.15	4.43

4. Conclusion

This paper presented an investigation of the interaction between the user hand and a dual-element UWB antenna array for mobile phones in three usage scenarios. The impact of the user hand on the antennas performance was studied in the frequency ranges 698-990 MHz and 1710-5530 MHz. The degree of influence depends on the antenna position with respect to the user's hand as well as the operating frequency. Due to the wideband performance of the antennas, the dielectric loading introduced by the hand causes not very significant changes in the antennas bandwidths and feeding efficiencies (include return loss and isolation). The main factor leading to a degradation of the total efficiency is the power absorption, studied by the absorption efficiency, as the presence of more human tissue in the antenna near field causes more severe problem. For an isotropic environment, the effect of user hand on the mean effective gain, branch power ratio, envelope correlation, diversity gain and multiplexing efficiency was studied. The hand proximity decreases the mean effective gain of the antennas and its different impact on them leads to branch power ratio different from 0 dB (gain imbalance) resulting in a deteriorated diversity gain. However, the reduction of the envelope correlation in the user presence at low frequencies enhances the diversity gain and also the multiplexing efficiency. In addition, the SAR of the antennas for all usage scenarios was determined.

5. References

[1] FCC 03-322 Federal Communications Commission, 'Facilitating opportunities for flexible, efficient, and reliable spectrum use employing cognitive radio technologies, notice of proposed rule making and order', December 2003

[2] Mitola, J., Maguire, G.Q.: 'Cognitive radios: making software radios more personal', IEEE Personal Commun., 1999,**6**, (4), pp. 13–18

[3] Haykin, S.: 'Cognitive radio: brain-empowered wireless communications', IEEE J. Sel. Areas Commun., 2005, **23**, (2), pp. 201–220

[4] Zhang, R., Liang, Y.-C.: 'Exploiting multi-antennas for opportunistic spectrum sharing in cognitive radio networks', IEEE J. Sel. Top. Signal Proc., 2008, **2**, (1), pp. 88–102

[5] Hussain, R., Sharawi, M.S.: 'A cognitive radio reconfigurable MIMO and sensing antenna system', IEEE Antennas Wireless Propag. Lett., 2015, **14**, pp. 257–260

[6] Tawk, Y., Costantine, J., Christodoulou, C.G.: 'Reconfigurable filtennas and MIMO in cognitive radio applications', IEEE Trans. Antennas Propag., 2014, **62**, (3), pp. 1074–1083

[7] Zamudio, M., Tawk, Y., Costantine, J., *et al.*: 'Integrated cognitive radio antenna using reconfigurable band pass filters', 5th Eur. Conf. Antennas Propag., Rome, Italy, April 2011, pp. 2108–2112

[8] Ren, Y.J.: 'Ceramic based small LTE MIMO handset antenna', IEEE Trans. Antennas Propag., 2013, **61**, (2), pp. 934-938

[9] Lee, J.-M., Kim, K.-B., Ryu, H.-K., *et al.*: 'A compact ultrawideband MIMO antenna with WLAN band-rejected operation for mobile devices', IEEE Antennas Wireless Propag. Lett., 2012, **11**, pp. 990-993

[10] Zhou, X., Quan, X., Li, R.: 'A dual-broadband MIMO antenna system for GSM/UMTS/LTE and WLAN handsets', IEEE Antennas Wireless Propag. Lett., 2012, **11**, pp. 551-554

[11] Li, J.-F., Chu, Q.-X., Huang, T.-G.: 'A compact wideband MIMO antenna with two novel bent slits', IEEE Trans. Antennas Propag., 2012, **60**, (2), pp. 482-489

[12] Yu, W., Yang, S., Tang, C.L., *et al.*: 'Accurate simulation of the radiation performance of a mobile slide phone in a hand-head position', IEEE Antennas Propag. Mag., 2010, **52**, (2), pp. 168–177

[13] Pelosi, M., Franek, O., Knudsen, M.B., *et al.*: 'Antenna proximity effects for talk and data modes in mobile phones', IEEE Antennas Propag. Mag., 2010, **52**, (3), pp. 15–26

[14] Kivekas, O., Ollikainen, J., Lehtiniemi T., *et al.*: 'Bandwidth, SAR, and efficiency of internal mobile phone antennas', IEEE Trans. Electromagn. Compat., 2004, **46**, (1), pp. 71-86

[15] Ilvonen, J., Valkonen, R., Holopainen, J., *et al.*: 'Reducing the interaction between user and mobile terminal antenna based on antenna shielding', 6th Eur. Conf. Antennas Propag., Prague, 2012, pp. 1889-1893

[16] IIvonen, J., Kivekas, O., Holopainen, J., *et al.*: 'Mobile terminal antenna performance with the users hand: Effect of antenna dimensioning and location', IEEE Antennas Wireless Propag. Lett., 2011, **10**, pp. 772–775

[17] Holopainen, J., Kivekas, O., IIvonen, J., *et al.*: 'Effect of the user's hands on the operation of lower UHF-band mobile terminal antennas: Focus on digital television receiver', IEEE Trans. Electromagn. Compat., 2011, **53**, (3), pp. 831–841

[18] Pelosi, M., Franek, O., Knudsen, M. B., *et al.*: 'Influence of dielectric loading on PIFA antennas in close proximity to user's body', Electronics Lett., 2009,**45**, (5), pp. 246-247

[19] Azremi, A.A.H., Ilvonen, J., Valkonen, *et al.*: 'Coupling element-based dual-antenna structures for mobile terminal with hand effects', Int. J. Wireless Inf. Netw., 2011, **18**, (3), pp. 146–157

[20] Plicanic, V., Lau, B.K., Derneryd, A., *et al.*: 'Actual diversity performance of a multiband diversity antenna with hand and head effects', IEEE Trans. Antennas Propag, 2009, **57**, (5), pp. 1547–1556

[21] Zhang, S., Zhao, K., Zhinong, Y., *et al.*: 'Adaptive quad-element multi-wideband antenna

array for user-effective LTE MIMO mobile terminals', IEEE Trans. Antennas Propag, 2013, **61**, (8), pp. 4275–4283

[22] Zhekov, S.S., Tatomirescu, A., Pedersen, G.F.: 'Compact multiband sensing MIMO antenna array for cognitive radio system', Loughborough Antennas and Propag. Conf., Loughborough, UK, November 2015, pp. 1–5

[23] 'Keysight' (formerly Agilent's Electronic Measurements), http://www.keysight.com

[24] 'Satimo', http://www.satimo.com/

[25] CTIA revision 3.4.2, 'Test plan for wireless device over-the-air performance', May 2015

[26] Valkonen, R. , Ilvonen, J., Rasilainen, K., *et al.*: 'Avoiding the interaction between hand and capacitive coupling element based mobile terminal antenna', 5th Eur. Conf. Antennas Propag., Rome, Italy, April 2011, pp. 2781-2785

[27] Gao, Y., Chen, X., Ying, Z., *et al.*: 'Design and performance investigation of a dual-element PIFA array at 2.5 GHz for MIMO terminal', IEEE Trans. Antennas Propag, 2007, **55**, (12), pp. 3433-3441

[28] Ilvonen, J., Kiveks, O., Azremi, A.A.H., *et al.*: 'Isolation improvement method for mobile terminal antennas at lower UHF band', 5th Eur. Conf. Antennas Propag., Rome, Italy, April 2011, pp. 1238-1242

[29] Tian, R., Lau, B.K., Ying, Z.: 'Multiplexing efficiency of MIMO antennas', IEEE Antennas Wireless Propag. Lett., 2011, **10**, pp. 183-186

[30] 'CST Microwave Studio', http://www.cst.com

[31] International commission on non-ionizing radiation protection (ICNIRP) 'Guidelines for limiting exposure to time-varying electric, magnetic, and electromagnetic fields (up to 300 GHz)', April 1998